

Porous Gelatin Hydrogels: 2. In Vitro Cell Interaction Study

Peter Dubruel,^{*,†,‡} R. Unger,[‡] Sandra Van Vlierberghe,[†] Veerle Cnudde,[§]
Patric J. S. Jacobs,[§] Etienne Schacht,[†] and C. J. Kirkpatrick[‡]

Polymer Chemistry and Biomaterials Research Group, Ghent University, Krijgslaan 281, Building S4 Bis, B-9000 Ghent, Belgium, Institute of Pathology, Johannes Gutenberg University, Langenbeckstrasse 1, D-55101 Mainz, Germany, and Department of Geology and Soil Science, Ghent University, Krijgslaan 281, Building S8, B-9000 Ghent, Belgium

Received July 14, 2006; Revised Manuscript Received September 22, 2006

We report on the feasibility of applying porous gelatin hydrogels, prepared by a novel and controlled cryogenic treatment, as cell-interactive scaffolds for tissue engineering applications. Despite the large number of publications on gelatin as a biomaterial, a detailed study of screening a limited number of gelatin scaffolds for their interaction with a panel of human cells has, to the best of our knowledge, not yet been published. In the present work, we have evaluated two types of porous gelatin scaffolds that differ in their pore geometry and pore size. Type I hydrogels contained top-to-bottom transverse channels (i.e. cones) with a decreasing diameter from the top (330 μm) to the bottom (20–30 μm). Type II hydrogels contained spherical pores with a diameter of 135 μm . Both types of scaffolds were evaluated by confocal laser scanning microscopy in terms of adhesion, spreading, and proliferation of human cells (endothelial, epithelial, fibroblast, glial, and osteoblast) by visualizing cells using calcein–acetoxymethyl ester as a vital stain. The results indicated that cells attached, spread, and proliferated on both types of hydrogels. In addition, the scaffolds developed can be used for the long-term culturing of human cells.

1. Introduction

Tissue engineering is still a relatively new research field in which principles and techniques from different research disciplines including material science, engineering, medicine, and cell and molecular biology are elegantly combined.¹ For years, a large number of candidate materials including polymers, metals, bioceramics, or composite materials have been developed and evaluated as (temporary) scaffolds for supporting and/or stimulating the formation of new tissues.² In the present work, we will evaluate the potential of porous gelatin-based hydrogels, prepared by a cryogenic treatment, as cell-interactive scaffolds for tissue engineering applications. Gelatins have previously found widespread applications as food ingredients (in meat, confectionery, beverages, etc), pharmaceutical capsules, tablet coatings, paper additives, cosmetic ingredients, or additives to photographic silver emulsions.³ In comparison to the above-mentioned examples, the application of gelatin for tissue engineering applications is a more recent development originating from the 1970s.⁴ In previous years, gelatin has been applied as biomaterials such as cell-interactive coatings or microcarriers embedded in other biomaterials. A nonexhaustive overview of the most recent publications, subdivided alphabetically by application, is summarized in Table 1. The table, based on a literature search in PubMed using gelatin and tissue engineering as keywords, clearly indicates that gelatin has a wide application range within the field of both soft and hard tissue engineering. In our opinion, however, the extensive data available on the application of gelatin as a biomaterial is very scattered. Different research groups have separately evaluated gelatin-based biomaterials that differ in the applied gelatin type,

cross-linking agent, additives (in the case of composites), pore size, pore geometry, and pore distribution.^{5–42} In addition, only a limited number of cell types have been included in most studies. This makes a meaningful understanding of how one type of (gelatin) scaffold with its specific properties can be applied as a suitable substrate for a variety of cell types rather difficult. The aim of the present paper is therefore to screen a limited number of porous gelatin-based scaffolds using a panel of different human cells. The scaffolds were developed using a recently described novel approach (cryogenic treatment in combination with an applied temperature gradient), enabling the production of scaffolds with elongated channels throughout the material.⁴³ In the present work, the adhesion, spreading, and proliferation of human cells on the porous gelatin hydrogels are evaluated by confocal microscopy visualization of calcein–acetoxymethyl ester (CAM)-labeled cells.

2. Materials and Methods

2.1. Hydrogel Synthesis. For this work, two types of porous gelatin hydrogels with varying pore geometry and pore size were evaluated. For the development of both hydrogels, methacrylamide-modified gelatin type B was used as a starting material. The gelatin applied was isolated from bovine skin by an alkaline process (Rousselot). The material had an approximate isoelectric point of 5 and a Bloom strength of 257.

The synthesis of methacrylamide-modified gelatin was performed as described earlier.⁴⁴ Part of the amine functions of gelatin were reacted with methacrylic anhydride. For this work, a derivative with a degree of substitution of 60%, based on the lysine and hydroxylysine units, was used.⁴⁴ In a subsequent step, the modified gelatin was used for the production of 10% (w/v) hydrogels.⁴³ Shortly, the hydrogels were obtained by dissolving 1 g of gelatin type B, previously modified with methacrylamide side groups, in 10 mL of double distilled water at 40 °C, containing 2 mol % photoinitiator Irgacure 2959 (Ciba specialty Chemicals N.V.), as calculated relative to the methacrylamide side chains.

* Author to whom correspondence should be addressed. Phone: 003292644466. Fax: 003292644972. E-mail: Peter.Dubruel@UGent.be.

[†] Polymer Chemistry and Biomaterials Research Group, Ghent University.

[‡] Institute of Pathology, Johannes Gutenberg University.

[§] Department of Geology and Soil Science, Ghent University.

Table 1. Overview of Biomedical Applications of Gelatin

application	type of gelatin	reference
adipose tissue	gelatin sponge	5
blood vessel	gelatin-grafted poly(ϵ -caprolactone) nanofibers, vascular endothelial	6–11
	growth factor immobilized gelatin, poly(ethylene glycol) diacrylate cross-linked gelatin, chitosan/gelatin blends, gelatin-grafted poly(ethylene terephthalate) nanofibers, gelatin-coated polyethersulfone fibers	
bone	hydroxyapatite chitosan/gelatin composite, gelatin-coated poly(α -hydroxy acids), glutaraldehyde cross-linked gelatin, hydroxyapatite/gelatin composite, β -tricalcium phosphate/gelatin composite, gelatin/poly(ϵ -caprolactone) blended nanofibers	12–19
cartilage	gelatin/chondroitin-6-sulfate/hyaluronan tri-copolymer, plasmid DNA immobilized chitosan/gelatin, gelatin microparticle embedded oligo(poly(ethylene glycol) fumarate) hydrogels, gelatin microparticle embedded poly(D,L-lactide- ϵ -caprolactone)	20–24
general	transglutaminase cross-linked gelatin, proanthocyanidin cross-linked chitosan gelatin, gelatin-coated poly(D,L-lactide), electrospun gelatin fibers, poly(3-hydroxybutyrate-co-3-hydroxyhexanoate)/gelatin blend, poly(vinyl alcohol)/gelatin blend, poly(<i>N</i> -isopropylacrylamide) grafted gelatin, gelatin- and fibronectin-coated polyelectrolyte multilayer nanofilms	25–33
heart	gelatin-coated polyurethane films	34
intervertebral disc	gelatin/chondroitin-6-sulfate/hyaluronan tri-copolymer, gelatin, glutaraldehyde cross-linked gelatin/chondroitin-6-sulphate	35–37
liver	cross-linked sodium alginate/gelatin	38
muscle	gelatin-grafted poly(ϵ -caprolactone) nanofibers	39
nerve	photo-cross-linkable gelatin	40
pancreas	gelatin-grafted agarose	41
skin	glutaraldehyde cross-linked gelatin	42

The solution was then injected into the mold of a cryo-unit, after which the solution was allowed to gel for 1 h at room temperature. In a final step, the hydrogel was exposed to UV light (276 nm, 10 mW/cm², Vilber Lourmat) for 2 h. Next, to induce different pore geometries and pore sizes within the hydrogels, different cryogenic treatments were applied as described in detail in a previous paper.⁴³ Both types of hydrogels were subjected to the same cooling regime (cooling range, 21 to -30 °C; cooling rate, 0.15 °C/min). For type I hydrogels, a temperature gradient (30 °C) between the top and the bottom of the scaffold was applied during the freezing step. Type II hydrogels were obtained without an applied temperature gradient. After incubation of the sample for 1 h at the final freezing temperature, the frozen hydrogel was transferred to a freeze-dryer to remove the ice crystals, resulting in a porous scaffold. The hydrogels were sterilized using ethylene oxide prior to cell seeding.

2.2. Hydrogel Pore Size and Pore Geometry Analysis. The visualization of both porous structures was performed using different techniques: microcomputed tomography (μ -CT), scanning electron microscopy (SEM), and optical microscopy.

For the μ -CT analysis, a “Skyscan 1072” X-ray microtomograph was used as described in detail previously.^{43,45–46} In brief, the system consisted of an X-ray shadow microscopic system and a computer with tomographic reconstruction software. The porous gelatin hydrogels were scanned at a voltage of 130 kV and a current of 76 μ A.

The porous scaffolds were also examined using SEM and optical microscopy. For the SEM analysis, a Fei Quanta 200F (field emission gun) scanning electron microscope was used for analysis of the gold-sputtered samples. For the optical microscopy pictures, an Axiotech 100 reflected light microscope (Carl Zeiss), with reflected light brightfield for Köhler illumination was used.

2.3. Cell Cultivation. The in vitro cell biocompatibility of both types of scaffolds was evaluated by applying a panel of human cells on the hydrogels: endothelial cells (human umbilical vein endothelial cells (HUVECs)), osteoblasts (MG-63 and CAL-72), human foreskin fibroblasts, glial cells (U373-MG), and epithelial cells (HELA). All cells used in this work were typically passaged twice weekly.

HUVECs were isolated from umbilical veins as described earlier by Jaffe et al.⁴⁷ The HUVECs were propagated in M199 medium (Sigma) supplemented with 20% fetal calf serum (FCS) (PAA), 1% penicillin/streptomycin (Gibco), 0.34% Glutamax (Gibco), 25 μ g/mL

endothelial cell growth factor (Beckton Dickinson), and 25 μ g/mL sodium heparin (Sigma-Aldrich) at 37 °C (5% CO₂) on gelatin-coated (Sigma-Aldrich, 0.2%) cell culture surfaces. All experiments were performed with cells in passage 2 or 3.

MG-63 and U373-MG were cultured in Eagle’s minimum essential medium (EMEM) (Sigma) supplied with 10% FCS, 1% penicillin/streptomycin (Gibco), and 1% Glutamax (Gibco) at 37 °C (5% CO₂).

CAL-72 and human foreskin fibroblasts were cultured in Dulbecco’s modified Eagle medium (DMEM) (Sigma) supplied with 10% FCS, 1% penicillin/streptomycin (Gibco), and 2% Glutamax (Gibco) at 37 °C (5% CO₂).

HELA cells were cultured in Roswell Park Memorial Institute (RPMI) medium (Gibco) supplied with 5% FCS, 1% penicillin/streptomycin (Gibco), and 1% Glutamax (Gibco) at 37 °C (5% CO₂).

2.4. Cell Seeding on the Hydrogels. Prior to cell seeding, the freeze-dried hydrogels were incubated in cell culture medium with serum for 2 h at room temperature. The swollen hydrogels were then cut with a scalpel to 15 mm \times 4 mm \times 3 mm cubes. For all experiments, the initial number of cells seeded on the biomaterial (15 mm \times 4 mm \times 3 mm) was 160 000. Cell seeding was performed by drop seeding. For type I hydrogels, cells were seeded at the site of the largest pores. To immerse the gelatin hydrogels completely with medium and thus to prevent them from floating, the hydrogels were “fixed” to the bottom of 6-well plates using silicone flexiPERM rings (Vivascience). The amount of medium required to prevent the flexiPERM rings (and thus the hydrogels) from floating was 3 mL. After 1 day, the flexiPERM rings were removed, and the hydrogel samples were transferred to a 12-well plate, flipped, and incubated with 2 mL of fresh medium. Culture medium was changed twice a week.

2.5. Cell Visualization within the Hydrogels. Cells seeded on the hydrogel were visualized within the gelatin hydrogels at different time points using confocal microscopy. Cell-seeded hydrogels were first incubated with CAM (1 μ g/mL) for 5–10 min at 37 °C in the dark. CAM is a cell-permeable compound that is taken up by viable cells and subsequently hydrolyzed by intracellular esterases. Upon hydrolysis, CAM becomes highly fluorescent and cell-impermeable, which makes it suited for vital cell visualization purposes. After the incubation step, the hydrogels were transferred into a Petri dish for confocal microscopy analysis (Leica TCS NT).

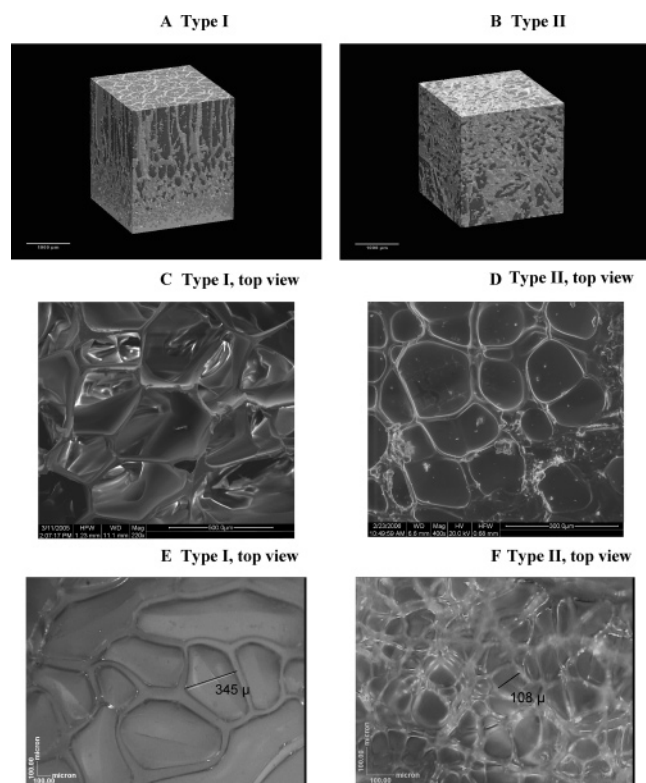


Figure 1. μ -CT, SEM, and optical microscopy analysis of type I and II gelatin hydrogels. Rows 1–3 represent μ -CT, SEM, and optical microscopy data for both types of porous hydrogels, respectively. For the μ -CT pictures (parts A and B), the pores are colored dark gray, and the scaffold material is light gray. The scale bars represent 1000 μ m (parts A and B), 500 μ m (part C), 300 μ m (part D), and 100 μ m (parts E and F).

3. Results and Discussion

In a recently published study, we described a novel method to produce porous gelatin scaffolds by applying a cryogenic treatment on chemically cross-linked hydrogels.⁴³ Variation of the cryogenic parameters applied enabled us to vary the pore size and pore geometry of the hydrogels, leading to hydrogels with either elongated channels or spherical pores throughout the entire material. In our opinion, our paper was the first report describing a controlled cryogenic treatment in which the application of a temperature gradient between the top and the bottom of the material during the freezing step resulted in (gelatin) hydrogels with a pore size gradient. In the present work, we wanted to test the *in vitro* biocompatibility of some of the materials developed.

3.1. Hydrogel Preparation and Characterization. Two different types of porous hydrogels were prepared by cryogenic treatment of cross-linked methacrylamide-modified gelatin. First, the modified gelatin was synthesized by reacting part of the lysine and hydroxylysine units of gelatin type B with methacrylic anhydride as described in detail in a previous paper.⁴⁴ The degree of substitution of the gelatin used in the present study was 60% (determination via ^1H NMR), based on the gelatin primary amine functions. Next, hydrogels were formed by gelation of an aqueous methacrylamide-modified gelatin solution, followed by radical cross-linking using a UV-active photoinitiator. Finally, the chemically cross-linked hydrogels were subjected to a cryogenic treatment. By varying the conditions of the cryogenic treatment, gels with different pore morphologies and sizes were obtained as outlined in detail in a previous paper.⁴³

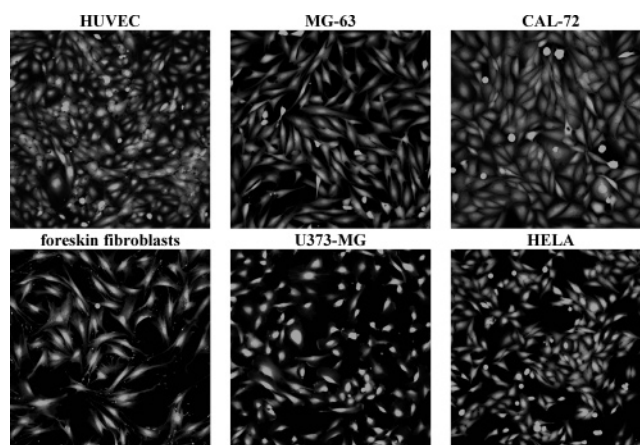


Figure 2. Visualization of tissue culture plastic (TCP) seeded with HUVECs, MG-63, CAL-72, foreskin fibroblasts, U373-MG, and HELA. For HUVECs, the TCP was precoated with gelatin. Cells were stained with CAM (1 μ g/mL) and visualized (20 \times magnification) using confocal microscopy.

The pore sizes and morphologies of the 3D scaffolds, which were selected for the *in vitro* biocompatibility study, were analyzed by μ -CT, SEM, and optical microscopy analysis. The μ -CT results, as shown in Figure 1 A, clearly indicated differences in pore size between the top and the bottom of type I scaffolds. Within the picture, which was a 3D reconstruction of the obtained 2D images, the light gray areas corresponded to the material, and the dark gray areas corresponded to the pores. The pore size decreased from the top (330 μ m) to the bottom of the material (20–30 μ m). The elongated channels present in the material were due to the applied temperature gradient (30 $^{\circ}\text{C}$) during the cryo-treatment.⁴³ The size of the spherical pores of type II hydrogels, as studied by μ -CT analysis (Figure 1B), was in the range of 135 μ m. The pore sizes and geometries of both types of scaffolds were further evaluated using SEM (Figures 1C and 1D) and optical microscopy (Figures 1E and 1F). Both techniques confirmed the data obtained by μ -CT analysis.

3.2. Cell Seeding on the Hydrogels. To evaluate to what extent the induced differences in pore size and geometry affected the interaction with cells, we performed an initial *in vitro* screening of both types of scaffolds using a panel of human cells from different organ tissue origins: endothelial cells (human umbilical vein endothelial cells, HUVEC), osteoblasts (MG-63 and CAL-72), human foreskin fibroblasts, glial cells (U373-MG), and epithelial cells (HELA). For this study we selected more cell lines rather than primary cells, since cell lines are reproducible from lab to lab. In addition, they exhibit many of the phenotypic markers of the primary cells that they represent. Primary cells show donor to donor variation and are more difficult to culture, and phenotype may vary from passage to passage and from lab to lab. Control pictures of the different cell types seeded on tissue culture plastic are shown in Figure 2.

3.3. Cell Survival and Organization on and within Type I Hydrogels. At different incubation times after cell seeding, the cells were stained using CAM as a vital stain. Using this stain, only vital cells are stained. This enabled a visualization of the cells and analysis of adhesion, spreading, and proliferation after seeding on the hydrogels. The results are summarized in Figures 3 and 4. For these preliminary experiments, cell visualization was performed on the same side of the scaffold on which the cells were seeded. Up to 3 days after cell seeding, most HUVECs show a rounded morphology, whereas only a minor portion of the individual endothelial cells were spread

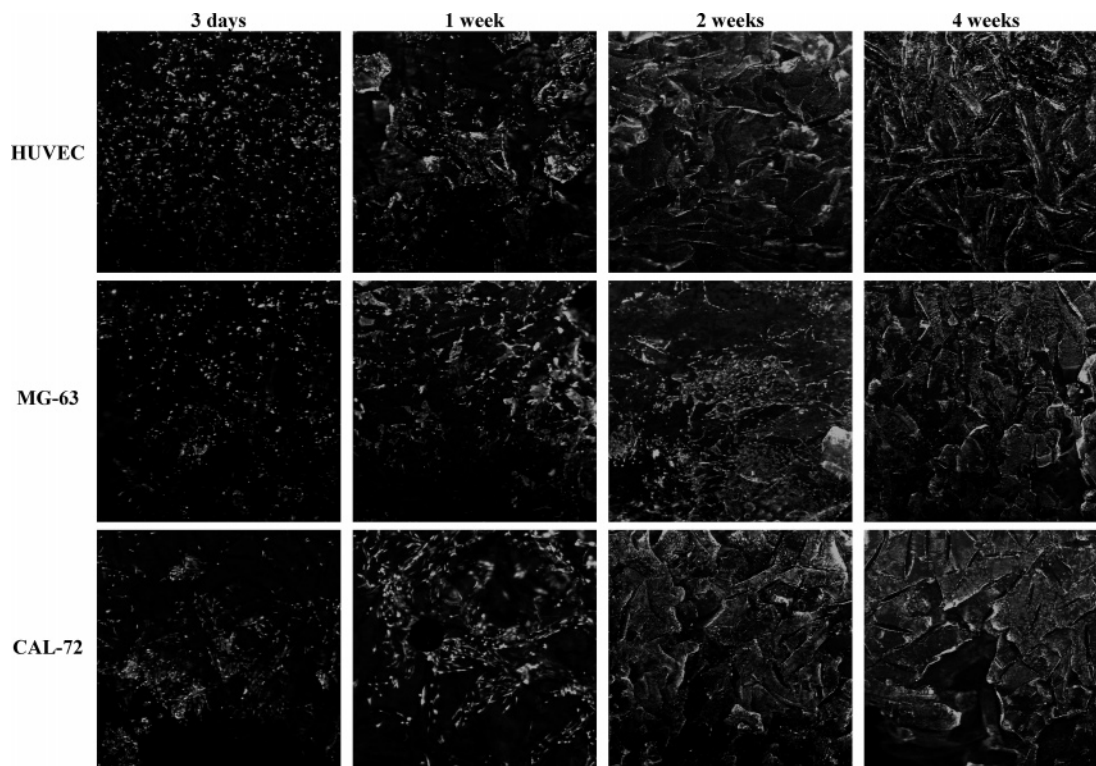


Figure 3. HUVEC, MG-63, and CAL-72 visualization (5 \times magnification) on type I porous gelatin hydrogels at different time points after cell seeding. Cells were stained with CAM (1 $\mu\text{g/mL}$) and visualized using confocal microscopy.

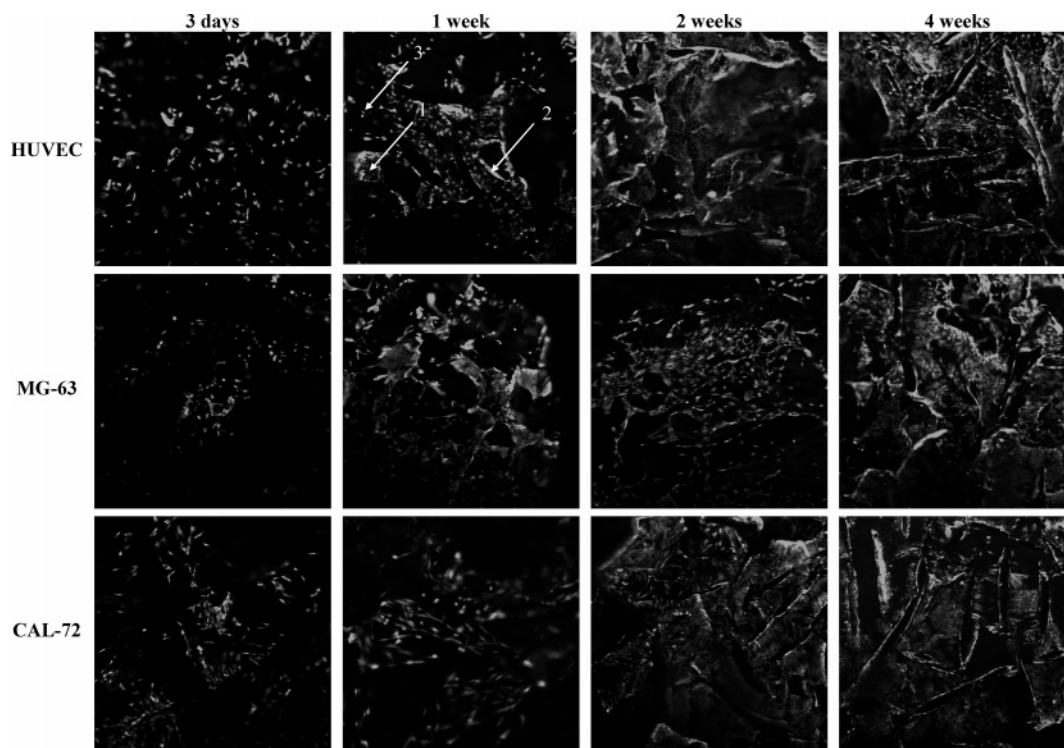


Figure 4. Magnification at 10 \times of the data represented in Figure 3.

out on the scaffolds. However, after 1 week, all cells had attached and spread-out cell morphology, and the formation of cell clusters was observed. Within the hydrogel, three different types of cellular organization could be distinguished as indicated by the numbered arrows in Figure 4. Part of the hydrogel was covered with confluent cell layers (arrow 1 in Figure 4). For endothelial cells, close cell–cell contacts are a requirement since these contacts control the permeability of the blood vessel wall,

forming a barrier for solutes, macromolecules, and leukocytes.⁴⁸ In other areas of the hydrogels, HUVECs formed aligned cell entities along the pores of the hydrogels (arrow 2 in Figure 4). Finally, in addition to the confluent cell layers and the cells aligned along the pores, a small number of single cells were also observed on the hydrogels (arrow 3 in Figure 4).

After longer incubation times on the porous gelatin scaffolds (> 1 week), the cell density on the scaffolds gradually increased.

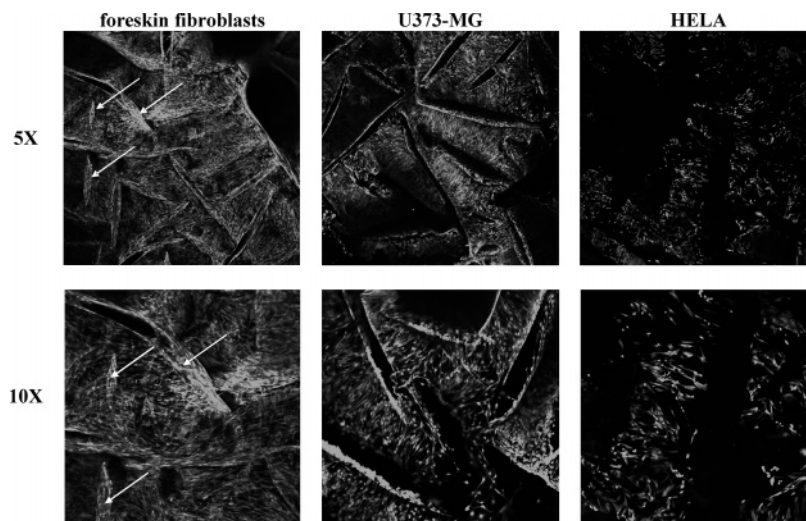


Figure 5. Visualization of foreskin fibroblasts, U373-MG, and HELA on type I hydrogels, 4 weeks after cell seeding. Cells were stained with CAM (1 $\mu\text{g/mL}$) and visualized using confocal microscopy.

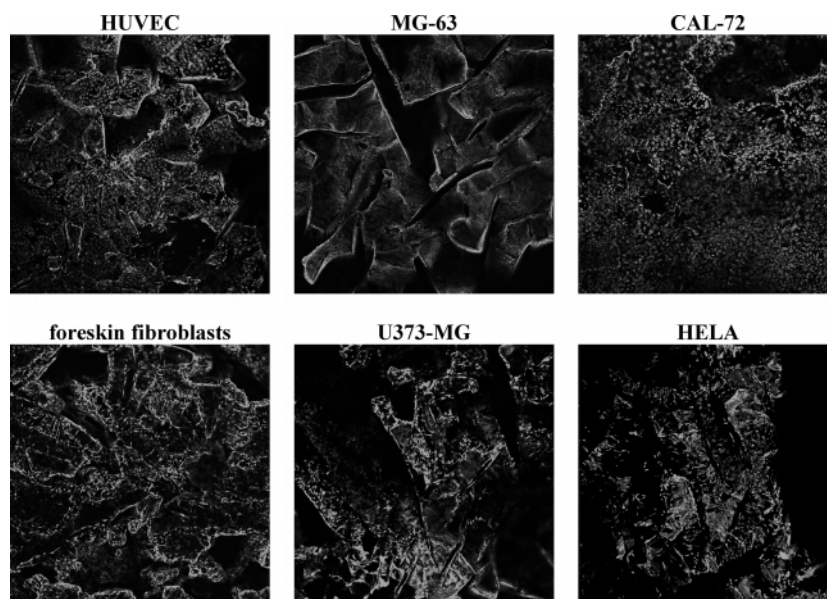


Figure 6. Cell visualization (5 \times magnification) on type II hydrogels, 4 weeks after cell seeding. Cells were stained with CAM (1 $\mu\text{g/mL}$) and visualized using confocal microscopy.

Dividing cells spread out to cover most of the available surface area and formed nearly confluent monolayers with cell–cell contacts. As a result of the cell proliferation on the material, only confluent cell layers and aligned cell entities appeared on the material whereas the number of isolated single cells decreased. These *in vitro* studies have shown that endothelial cells remained viable for at least 4 weeks on the hydrogels. Currently, we are further evaluating the potential of these hydrogels for long-term culturing of endothelial cells, which would have important applications in the field of bioreactor technology.

From the examination of the cell organization on the structures (Figures 3 and 4) compared to the induced pore size and geometry, as visualized by μ -CT, SEM, and optical microscopy (Figure 1), it could be concluded that with an increasing incubation time the endothelial cells nearly covered all of the available hydrogel surfaces without bridging the pores within the hydrogel structure. In those areas where pores were present, endothelial cells aligned along the pore. At present, we are performing further studies to determine to what extent endothelial cells have the ability to grow into the pores of the

scaffolds with time. Preliminary results indicated that HUVECs indeed grow into the pores of the scaffolds developed (data not shown).

In comparison to cell seeding on gelatin-coated cell culture flasks, the attachment and spreading of endothelial cells on the hydrogels was much slower. Endothelial cells adhered and spread on gelatin-coated cell culture plastic within 1–2 h. Most likely, these differences could be ascribed to the 3D character of the porous scaffolds. Upon cell seeding, the endothelial cells were not in contact with a flat polymer surface but rather with a complex 3D porous hydrogel. More steps may be involved in the attachment and spreading to the hydrogels in comparison to attachment on flat cell culture flasks which was favored by gravity. This may explain the slower attachment and spread on the 3D materials.

For MG-63 osteoblasts, similar results were observed in terms of cell adhesion and spreading as were observed with HUVECs. Up to 3 days after cell seeding, MG-63 cells showed a rounded morphology (Figures 3 and 4). After longer incubation times, cells started to spread out and proliferate, covering the entire scaffold surface. In contrast to HUVEC-seeded hydrogels, MG-

63 cells mainly formed confluent cell layers after two weeks of incubation. After four weeks in vitro, the number of aligned cell entities increased slightly. Since type I hydrogels from the same batch were used for both sets of experiments, we are presently investigating the differences observed in cell alignment between these two cell types.

In contrast with the results obtained for HUVECs and MG-63 cells, CAL-72 cells adhered and spread on the porous gelatin hydrogels within 3 days after cell seeding (Figures 3 and 4). The cell behavior after longer incubation times was similar to that of HUVECs.

In addition to endothelial cells and osteoblasts, we also screened type I hydrogels for the growth of human foreskin fibroblasts, glial cells (U373-MG), and epithelial cells (HELA). The results after 4 weeks of incubation, as summarized in Figure 5, clearly indicate that the porous gelatin scaffolds were an excellent candidate material for the (long-term) culturing of these cell types also, and the hydrogels are thus an excellent substrate for a large variety of human cells. It should be mentioned that, in contrast to the other cell types studied, human foreskin fibroblasts bridged the hydrogel pores in some areas after 4 weeks of incubation (arrows in Figure 5, first column). Most likely, this can be ascribed to the high amount of extracellular matrix produced by these cells on the scaffolds.⁴⁹

3.4. Cell Survival and Organization on and within Type II Hydrogels. Since it is well-known that differences in both surface chemistry and surface topography affect the interaction with cells,⁵⁰ we were interested in investigating to what extent differences in pore size and pore geometry within gelatin scaffolds with the same surface chemistry would affect the cell interaction. Type I and II gelatin hydrogels were both developed starting from type B methacrylamide-modified gelatin. Variation of the parameters used for cryogenic treatment leads to variations in pore geometry and pore size between the two scaffold types without altering the scaffold chemical composition.

The same panel of cells as described above was also seeded on gelatin hydrogels with spherical pores (135 μm in diameter, type II hydrogels). The results for the different cell types after 4 weeks of incubation are summarized in Figure 6. It was concluded that type II scaffolds possessed similar properties in comparison to type I hydrogels in terms of cell attachment, spreading, and proliferation on the material. After cell seeding, the complete hydrogel surface was covered with an increasing incubation time. It should be noted that CAL-72 osteoblasts did not show the very bright and sharp CAM staining as observed for all other cell types. At present we are investigating these phenomena, but our preliminary data indicate that mineralization occurs at 4 weeks postseeding (Supporting Information). The mineralization process might have an effect on the CAM staining of cells embedded in the hydrogel.

The comparative data obtained for both types of hydrogels suggested that the pore geometry and pore size of the matrix did not affect the adhesion, spreading, and proliferation of cells, at least in the pore size and geometry range investigated in the present work. This could be concluded since the same type of gelatin (methacrylamide-modified gelatin type B) was used for the production of both scaffold types. The good cell-interactive properties of both types of porous gelatin hydrogels were not unexpected, since type B gelatin was obtained by alkaline denaturation of collagen, one of the components of the extracellular matrix. Chemical modification of gelatin, by derivatization of the ϵ -lysine amines with methacrylamide functions and subsequent cross-linking into a 3D network, did not affect (or at least not to a great extent) the cell-interactive properties

of the material. In addition, both types of gelatin hydrogels developed were highly porous. Preliminary results indicate that this property favors cell ingrowth and cell migration throughout the scaffold. The migration of cells throughout the scaffolds, which is required for tissue engineering applications, is presently under investigation in our laboratories and will be the subject of a subsequent paper.

4. Conclusions

In the present paper, we have screened two types of porous gelatin hydrogels for their interaction with a panel of human cells. We have shown that both types of gelatin scaffolds, differing in their pore geometry and pore size, supported the attachment and growth of human cells over longer time periods. We are currently further evaluating and screening the material for different applications. A first step in this direction is a series of in vivo animal studies to study possible effects of the chemical derivatization of gelatin on its immunological properties.

Acknowledgment. P.D. thanks the Alexander von Humboldt Foundation for financial support in the form of a Research Fellowship. The University of Ghent authors thank the Institute for the Promotion of Innovation by Science and Technology in Flanders, Belgium, and the Belgian Research Policy Inter University Attraction Poles (IUAP/PAI-V/03) for financial support. Anne Sartoris and Barbara Malenica are greatly acknowledged for their excellent technical assistance.

Supporting Information Available. Calcification in the gelatin hydrogels. This material is available free of charge via the Internet at <http://pubs.acs.org>.

References and Notes

- (1) Ma, P. X. *Mater. Today* **2004**, 7 (5), 30–40.
- (2) Hench, L. L.; Polak, J. M. *Science* **2002**, 295 (5557), 1014–1017.
- (3) Gelatin Manufacturers Institute of America Home Page. <http://www.gelatin-gmia.com/>, 2005.
- (4) Borras, A.; Meerhoff, A. *Am. J. Ophthalmol.* **1972**, 73 (3), 390–398.
- (5) Hong, L.; Peptan, I.; Clark, P.; Mao, J. J. *Ann. Biomed Eng.* **2005**, 33 (4), 511–517.
- (6) Ma, Z.; He, W.; Yong, T.; Ramakrishna, S. *Tissue Eng.* **2005**, 11 (7–8), 1149–1158.
- (7) Ito, Y.; Hasuda, H.; Terai, H.; Kitajima, T. *J. Biomed. Mater. Res., Part A* **2005**, 74 (4), 659–665.
- (8) Mironov, V.; Kasyanov, V.; Shu, X. Z.; Eisenberg, C.; Eisenberg, L.; Gonda, S.; Trusk, T.; Markwald, R. R.; Prestwich, G. D. *Biomaterials* **2005**, 26 (36), 7628–7635.
- (9) Huang, Y.; Onyeri, S.; Siewe, M.; Moshfeghian, A.; Madhally, S. V. *Biomaterials* **2005**, 26 (36), 7616–7627.
- (10) Ma, Z.; Kotaki, M.; Yong, T.; He, W.; Ramakrishna, S. *Biomaterials* **2005**, 26 (15), 2527–2536.
- (11) Unger, R. E.; Huang, Q.; Peters, K.; Protzer, D.; Paul, D.; Kirkpatrick, C. J. *Biomaterials* **2005**, 26 (14), 1877–1884.
- (12) Zhao, F.; Grayson, W. L.; Ma, T.; Bunnell, B.; Lu, W. W. *Biomaterials* **2006**, 27 (9), 1859–1867.
- (13) Liu, X.; Won, Y.; Ma, P. X. *J. Biomed. Mater. Res., Part A* **2005**, 74 (1), 84–91.
- (14) Yang, S. H.; Hsu, C. K.; Wang, K. C.; Hou, S. M.; Lin, F. H. *J. Biomed. Mater. Res., Part B* **2005**, 74 (1), 468–475.
- (15) Kim, H. W.; Kim, H. E.; Salih, V. *Biomaterials* **2005**, 26 (25), 5221–5230.
- (16) Kim, H. W.; Knowles, J. C.; Kim, H. E. *J. Biomed. Mater. Res., Part A* **2005**, 72 (2), 136–145.
- (17) Takahashi, Y.; Yamamoto, M.; Tabata, Y. *Biomaterials* **2005**, 26 (23), 4856–4865.
- (18) Takahashi, Y.; Yamamoto, M.; Tabata, Y. *Biomaterials* **2005**, 26 (17), 3587–3596.
- (19) Zhang, Y.; Ouyang, H.; Lim, C. T.; Ramakrishna, S.; Huang, Z. M. *J. Biomed. Mater. Res., Part B* **2005**, 72 (1), 156–165.

- (20) Chang, C. H.; Kuo, T. F.; Lin, C. C.; Chou, C. H.; Chen, K. H.; Lin, F. H.; Liu, H. C. *Biomaterials* **2006**, 27 (9), 1876–1888.
- (21) Guo, T.; Zhao, J.; Chang, J.; Ding, Z.; Hong, H.; Chen, J.; Zhang, J. *Biomaterials* **2006**, 27 (7), 1095–1103.
- (22) Park, H.; Temenoff, J. S.; Holland, T. A.; Tabata, Y.; Mikos, A. G. *Biomaterials* **2005**, 26 (34), 7095–7103.
- (23) Holland, T. A.; Bodde, E. W.; Baggett, L. S.; Tabata, Y.; Mikos, A. G.; Jansen, J. A. *J. Biomed. Mater. Res., Part A* **2005**, 75 (1), 156–167.
- (24) Holland, T. A.; Tabata, Y.; Mikos, A. G. *J. Controlled Release* **2005**, 101 (1–3), 111–125.
- (25) Ito, A.; Mase, A.; Takizawa, Y.; Shinkai, M.; Honda, H.; Hata, K.; Ueda, M.; Kobayashi, T. *J. Biosci. Bioeng.* **2003**, 95 (2), 196–199.
- (26) Broderick, E. P.; O'Halloran, D. M.; Rochev, Y. A.; Griffin, M.; Collighan, R. J.; Pandit, A. S. *J. Biomed. Mater. Res., Part B* **2005**, 72 (1), 37–42.
- (27) Kim, S.; Nimni, M. E.; Yang, Z.; Han, B. *J. Biomed. Mater. Res., Part B* **2005**, 75 (2), 442–450.
- (28) Zhu, H.; Ji, J.; Shen, J. *J. Biomater. Sci., Polym. Ed.* **2005**, 16 (6), 761–774.
- (29) Li, M.; Mondrinos, M. J.; Gandhi, M. R.; Ko, F. K.; Weiss, A. S.; Lelkes, P. I. *Biomaterials* **2005**, 26 (30), 5999–6008.
- (30) Wang, Y. W.; Wu, Q.; Chen, G. Q. *Biomacromolecules* **2005**, 6 (2), 566–571.
- (31) Cascone, M. G.; Lazzeri, L.; Sparvoli, E.; Scatena, M.; Serino, L. P.; Danti, S. *J. Mater. Sci.: Mater. Med.* **2004**, 15 (12), 1309–1313.
- (32) Ohya, S.; Nakayama, Y.; Matsuda, T. *J. Artif. Organs.* **2004**, 7 (4), 181–186.
- (33) Li, M.; Mills, D. K.; Cui, T.; Mcshane M. J. *IEEE Trans. Nanobiosci.* **2005**, 4 (2), 170–179.
- (34) Alperin, C.; Zandstra, P. W.; Woodhouse, K. A. *Biomaterials* **2005**, 26 (35), 7377–7386.
- (35) Yang, S. H.; Chen, P. Q.; Chen, Y. F.; Lin, F. H. *Artif. Organs.* **2005**, 29 (10), 806–814.
- (36) Brown, R. Q.; Mount, A.; Burg, K. J. *J. Biomed. Mater. Res., Part A* **2005**, 74 (1), 32–39.
- (37) Yang, S. H.; Chen, P. Q.; Chen, Y. F.; Lin, F. H. *J. Biomed. Mater. Res., Part B* **2005**, 74 (1), 488–494.
- (38) Balakrishnan, B.; Jayakrishnan, A. *Biomaterials* **2005**, 26 (18), 3941–3951.
- (39) Williamson, M. R.; Adams, E. F.; Coombes, A. G. *Biomaterials* **2006**, 27 (7), 1019–1026.
- (40) Gamez, E.; Goto, Y.; Nagata, K.; Iwaki, T.; Sasaki, T.; Matsuda, T. *Cell Transplant.* **2004**, 13 (5), 549–564.
- (41) Bloch, K.; Lozinsky, V. I.; Galaev, I. Y.; Yavriyantz, K.; Vorobeychik, M.; Azarov, D.; Damshkaln, L. G.; Mattiasson, B.; Vardi P. *J. Biomed. Mater. Res., Part A* **2005**, 75 (4), 802–809.
- (42) Witte, R. P.; Kao, W. J. *Biomaterials* **2005**, 26 (17), 3673–3682.
- (43) Van Vlierberghe, S.; Cnudde, V.; Dubruel, P.; Masschaele, B.; Cosijns, A.; De Paepe, I.; Jacobs, P. J. S.; Van Hoorebeke, L.; Remon, J. P.; Schacht, E. *Biomacromolecules* **2007**, 8 (2), 331–337.
- (44) Van den Bulcke, A.; Bogdanov, N.; De Rooze, N.; Schacht, E.; Cornelissen, M.; Berghmans, H. *Biomacromolecules* **2000**, 1 (1), 31–38.
- (45) Cnudde, V.; Jacobs, P. J. S. In *Proceedings of the International Workshop on X-ray CT for Geomaterials, GeoX2003*, Kumamoto, Japan, Nov 2003; Otani, J., Obara, Y., Eds.; A. A. Balkema: Leiden, Netherlands, pp 363–371, 2004.
- (46) Steppe, K.; Cnudde, V.; Girard, C.; Lemeur, R.; Cnudde, J. P.; Jacobs, P. J. *Struct. Biol.* **2004**, 148 (1), 11–21.
- (47) Jaffe, E. A.; Nachman, R. L.; Becker, C. G.; Minick, C. R. *J. Clin. Invest.* **1973**, 52 (11), 2745–2756.
- (48) Vestweber, D. *J. Pathol.* **2000**, 190 (3), 281–291.
- (49) Houglum, P. A. *Therapeutic Exercise for Musculoskeletal Injuries*, 2nd ed.; Human Kinetics: Champaign, IL, 2005.
- (50) Curtis, A.; Wilkinson, C. *Biomaterials* **1997**, 18 (24), 1573–1583.

BM0606869